

## Electrodeposition of granular FeCoNi films with large permeability for microwave applications

Bao-Yu Zong,<sup>\*a</sup> Zhuang-Wen Pong,<sup>b</sup> Yu-Ping Wu,<sup>c</sup> Pin Ho,<sup>a</sup> Jin-Jun Qiu,<sup>a</sup> Ling-Bing Kong,<sup>c</sup> Li Wang<sup>a</sup> and Gu-Chang Han<sup>a</sup>

Received 19th July 2011, Accepted 8th August 2011

DOI: 10.1039/c1jm13398e

A simple methodology to fabricate soft magnetic FeCoNi granular films from cheap salt solutions *via* electrodeposition at room temperature is demonstrated. With the addition of a small quantity of organic and inorganic additives into the solutions, the FeCoNi nano-granular films possess ultra-high permeability, large resistivity, and other desirable magnetic properties for gigahertz microwave applications. Typically, the films have a coercivity of less than 10 or 20 Oe along the hard or easy axis, respectively, with a saturation flux density of up to 2.43 T. The magnetic permeability and resistivity are correspondingly up to a magnitude order of about  $10^3$  and  $10^{-4}$   $\Omega$  cm. These soft FeCoNi films also show a big anisotropic field of more than 50 Oe and a very small magnetostriction of  $<10^{-5}$ . They can be potentially applied to microwave absorption as well as other applications.

## 1. Introduction

Magnetic soft materials possessing high microwave permeability are useful for high frequency microwave applications.<sup>1–3</sup> Currently, they are widely used in commercial and military devices, such as domestic microwave ovens, satellites, mobile phones, messaging apparatuses, palmtops, organizers, as well as fighter planes, rockets, and warships *via* military stealth technology.<sup>4–6</sup> For the construction of these highly compact, precise or mobile devices, thin-films instead of bulk absorbers are required.<sup>1,7,8</sup> To achieve this type of thin soft magnetic film, different sputtering systems are usually employed.<sup>9–11</sup> However, such systems are expensive and possess a limited chamber space due to the stringent requirement of very high vacuum (*e.g.*  $<10^{-6}$  Pa). As such, they are deemed unsuitable for mass production of large area films for microwave absorbers. In order to solve this issue, ferrite powders and composites have been developed.<sup>12–14</sup> For these materials, the issue lies in the complex and large energy-consuming processes, which are required for the preparing and coating the materials on the device surfaces. For instance, the powders have to be ground to small particles with uniform size, calcined or sintered at high temperature ( $>500$  °C) in non-air ambiance, and mixed with special adhesives before coating.<sup>13,15</sup> Thus, the search for a simple and low cost method, which can mass-produce large areas of thin films with high permeability ( $\mu$ ) as well as other desirable properties [*e.g.*, high saturation flux density (magnetization) ( $B_s$ ), resonance frequency

( $f_r$ ), anisotropy field ( $H_k$ ), resistivity ( $\rho$ ), low coercivity ( $H_c$ ), *etc.*] is interesting and demanded. Electrodeposition is a simple, cheap, and quick method for thin magnetic film preparation.<sup>16</sup> It can also prepare large area films with various compositions and morphologies. Furthermore, it also allows the films to be deposited on substrates of different shapes or materials.<sup>17</sup> Therefore, the use of this simple electrodeposition tool can greatly reduce the cost of commercial and military equipment. However, despite the large number of soft magnetic films fabricated using this tool<sup>18–21</sup> and attractive progresses achieved (such as ultra-high  $B_s$  films<sup>22–25</sup> and large magnetic permeability<sup>26</sup> or frequency<sup>27</sup> alloys have been prepared for magnetic recording devices), there has been few films prepared for more microwave applications (*e.g.* microwave absorption). In addition, the limited films reported for this function have either a low magnetic permeability ( $\mu < 50$ )<sup>27,28</sup> and resonance frequency ( $f_r < 1$  GHz),<sup>29</sup> or a low anisotropy field ( $H_k \leq 25$  Oe)<sup>22–25</sup> and resistivity ( $\rho < 10^{-5}$   $\Omega$  cm<sup>2</sup>),<sup>18</sup> as it is a great challenge to achieve a film possessing high resistivity  $\rho$ , large permeability  $\mu$  and anisotropy  $H_k$ , as well as high resonance frequency  $f_r$  simultaneously *via* electrodeposition.<sup>18,28</sup> Some groups report using metal nanowires electrodeposited as granular films for increasing the resistivity but this type of film only has a low  $\mu$  (usually  $<50$ ). Moreover, porous membranes have to be used for the preparation of the nanowires.<sup>28,29</sup>

In this work, FeCoNi-based films with ultra-high permeability are directly prepared through electrodeposition *via* careful selection of additives and plating parameters. The morphology and property of the deposited film can be tuned with different organic and inorganic additives. The uniform nano-columnar granular films (with large permeability) possess a higher resistivity in comparison to other granular films with different morphologies.

<sup>a</sup>Data Storage Institute, DSI Building, 5 Engineering Drive 1, Singapore, 117608, Republic of Singapore. E-mail: zong\_baoyu@dsi.a-star.edu.sg; Fax: +65 6777 1349; Tel: +65 6874 8411

<sup>b</sup>National Junior College, 37 Hillcrest Road, Singapore 288913

<sup>c</sup>Temasek Laboratories, National University of Singapore, #09-02, 5A Engineering Drive 1, Singapore 117411

## 2. Experimental

FeCoNi-based films were electrodeposited on glass and SiO<sub>2</sub> wafer substrates. A thin seed layer with the structure of Ta (10 nm)/FeCo(110) (20–30 nm) was first sputtered on the non-conductive substrates as an electrical conducting layer for the subsequent electrodeposition process. It is noted that electroless-deposition can be alternatively used for large area seed-layer deposition. The FeCoNi-based films were fabricated at room temperature from a cheap solution containing 0.114 M FeCl<sub>2</sub>, 0.153 M CoCl<sub>2</sub>·6H<sub>2</sub>O, 0.011 M NiCl<sub>2</sub>·6H<sub>2</sub>O, 0.010 M NiSO<sub>4</sub>·6H<sub>2</sub>O, 0.94 M NH<sub>4</sub>Cl, 1.0 M H<sub>3</sub>BO<sub>3</sub>, and different additives. First, a little organic sodium dodecyl sulfate (SDS) surfactant (1.1 g l<sup>-1</sup>) was added to the plating solution for enhancing the wettability of the substrates. Next, a suitable small quantity (5–15 g l<sup>-1</sup>) of organic dimethylamine borane [(CH<sub>3</sub>)<sub>2</sub>NHBH<sub>3</sub>, *B*-reducer] was dissolved in the solution to increase the saturation flux density *B<sub>s</sub>*, permeability  $\mu$ , and anisotropy *H<sub>k</sub>*, as well as to decrease the coercivity *H<sub>c</sub>* of the resultant films. Lastly, a little inorganic additive (1.0 g l<sup>-1</sup> AlK (SO<sub>4</sub>)<sub>2</sub> or 2.2 g l<sup>-1</sup> MnCl<sub>2</sub>) was mixed into the solution for improving the resistivity  $\rho$  of the film by changing the particle morphology in the films from granular to columnar. The electroplating current density was controlled within the range of 1.8–50 mA cm<sup>-2</sup>. The electroplating system used was a 1.2 or 57 l Paddle-Cell with DC power supply. During the electrodeposition of the FeCoNi films with a thickness from 100 nm to 1.2  $\mu$ m, a magnetic field of 280–300 Oe was applied parallel to the substrate surface to induce an in-plane uniaxial anisotropy.

The morphologies and thicknesses of the films were measured using an Atomic Force Microscope (AFM) and Field Emission Scanning Electron Microscope (FESEM). The stoichiometry of the electrodeposited films was determined by the Energy Dispersive X-ray (EDX), which was attached to the FESEM. For *B<sub>s</sub>* and coercivity (*H<sub>c</sub>*) measurements, a vibrating sample magnetometer (VSM, EV-7) was used. All the measurement methods were the same as previously reported.<sup>16</sup> The saturation flux density *B<sub>s</sub>* values were calculated from the formula  $B_s(T) = \mu_0 M_s = 4\pi \times 10^{-4} M$  (emu)/film volume (cm<sup>3</sup>), where *M* refers to the saturated magnetic moment in the *M*–*H* loop. The crystallographic texture of the films was evaluated from X-ray diffraction (XRD) by using a Philips X'pert diffractometer [ $\lambda = 1.5406$  Å, Bragg–Brentano geometry, PW3088/60 (line focus) Cu MRD PFX mirror, without a filter and a monochromator] and recorded at a scanning rate of 0.02° s<sup>-1</sup> in the  $2\theta$  ranging from 25 to 95°. The bulk resistivity  $\rho$  of the film, calculated from sheet resistance by dividing the film thickness, was measured using a four point probe head (RT-70). The permeability frequency spectra from 0.1 to 4 or 7 GHz were characterized with a vector network analyzer (Agilent 5230A), using a shorted micro-strip transmission-line perturbation fixture.<sup>30</sup>

## 3. Results and discussion

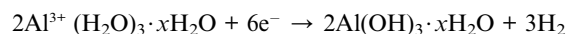
The FeCoNi-based nano-/micro-films with large permeability were cost-effectively prepared *via* electrodeposition using selected organic and inorganic additives in the plating solutions. The properties of the films largely depended on the additive type and concentration as well as the plating current density.

### 3.1 Effects on the film property for organic and inorganic additives

As for microwave applications in the gigahertz (GHz) range, magnetic films with low coercivity *H<sub>c</sub>*, high saturation flux density *B<sub>s</sub>* and permeability  $\mu$  are required, hence FeCoNi based materials, which possess the highest *B<sub>s</sub>* (up to 2.45 T theoretically), were chosen for the preparation of the required thin films. However, it was observed experimentally that the FeCoNi films deposited from a usual salt solution without any additive, typically possessed large *H<sub>c</sub>* (>40 Oe), low *B<sub>s</sub>* (<1.5 T), high magneto-crystalline anisotropy and magnetostriction ( $\lambda_s > 10^{-4}$ ), which were similar to the sputtered films.<sup>31,32</sup> For soft magnetic films, high permeability benefits from those possessing a high saturation flux density *B<sub>s</sub>*.<sup>2</sup> In our previous work, high *B<sub>s</sub>* and low *H<sub>c</sub>* films were obtained using the organic *B*-reducer as an additive in the plating solution.<sup>33</sup> However, the resultant films were verified to have a relatively low resistivity (<10<sup>-5</sup> Ω cm), making them unsuitable for microwave applications in the high frequency (GHz) range.<sup>2</sup> Hence in this work, FeCoNi films were electrodeposited using different organic and inorganic additives in the plating solution. In the initial make-up of the plating solution, a small quantity (1.1 g l<sup>-1</sup>) of organic SDS surfactant was added. Through the reduction of surface tension between the substrate and the plating solution, SDS largely increased the deposition coverage of the films on the substrates as well as widened the range of the current density during electroplating. In addition, SDS also slightly reduced the *H<sub>c</sub>* of the films as illustrated in Table 1. *B*-Reducer [(CH<sub>3</sub>)<sub>2</sub>NHBH<sub>3</sub>] was then used to increase *B<sub>s</sub>* as well as further decrease *H<sub>c</sub>* of the films. Being an effective reductant,<sup>34</sup> it can prevent Fe<sup>2+</sup> from oxidizing (Fe<sup>3+</sup> + e<sup>-</sup>  $\xrightarrow{B\text{-reducer}}$  Fe<sup>2+</sup>) in the plating solution.<sup>25</sup> It is also an effective additive for uniform deposition by reducing the particle size of the deposited film and improving the potential of the cathode (substrate) *via* cathode polarization.<sup>33</sup> By optimizing the concentration of *B*-reducer and the plating parameters, very magnetically soft FeCoNi films with high *B<sub>s</sub>* were prepared. In order to obtain both high *B<sub>s</sub>* and low *H<sub>c</sub>* values, larger atomic ratios (40–60%) of Fe (*B<sub>s</sub>* = 2.2 T)<sup>1,22</sup> and Co (*B<sub>s</sub>* = 1.8 T), and lower ratio (1–5%) of Ni (*B<sub>s</sub>* = 0.6 T) in the films were maintained by using the optimized salt concentrations and the current density range (12–35 mA cm<sup>-2</sup>). With the suitable electrodeposition parameters, coupled with the appropriate addition of *B*-reducer (6–10 g l<sup>-1</sup>), the coercivities in both the hard (*H<sub>c-hard</sub>*) and easy (*H<sub>c-easy</sub>*) axes could be reduced to less than 10 Oe, while the saturation flux density was increased to 1915 emu cm<sup>-3</sup> (~2.40 T), as shown in Fig. 1a and 2a. The relationship between the microwave permeability and the *B*-reducer concentration or plating parameters was further investigated. The characteristic results (depicted in Fig. 1b and 2b) demonstrate that an effective decrease in *H<sub>c</sub>* and improvement in *B<sub>s</sub>* of the film were accompanied by a large increase in the microwave permeability  $\mu$ . Thus, the addition of *B*-reducer in suitable quantity and the electrodeposition at a moderate current density not only largely decreased *H<sub>c</sub>* and increased *B<sub>s</sub>* but also significantly improved the microwave permeability  $\mu$  of the deposited films. However, excessive addition of *B*-reducer (>15 g l<sup>-1</sup>) or too high current density (>60 mA cm<sup>-2</sup>) produced an unstable plating solution or a burnt rough film, which resulted in the reduction in *B<sub>s</sub>* and  $\mu$ .

Upon achieving significant improvements in the magnetic permeability and other properties of the deposited thin films *via* the addition of SDS and *B*-reducer, the resistivity  $\rho$  of the film was further improved by the addition of inorganic  $\text{Al}^{3+}$  and  $\text{Mn}^{2+}$  additives through obtaining uniform nano-columnar granular films. Nano-columnar films in a uniform manner were expected to have larger resistivities, which can cater to the requirements of GHz microwave absorption.<sup>1</sup> In the acidic plating solution,  $\text{Al}^{3+}/\text{Al}$  (−1.7 V) and  $\text{Mn}^{2+}/\text{Mn}$  (−1.0 V) have much lower electrodeposition potentials compared to those of  $\text{Fe}^{2+}/\text{Fe}$  (−0.4 V),  $\text{Co}^{2+}/\text{Co}$  (−0.3 V), and  $\text{Ni}^{2+}/\text{Ni}$  (−0.2 V).<sup>19</sup> Hence when  $\text{Fe}^{2+}$ ,  $\text{Co}^{2+}$ , and  $\text{Ni}^{2+}$  were co-deposited into the FeCoNi alloy, only a small number of Al and Mn atoms might be doped in the alloy film. As Al and Mn

are very active metals in aqueous solutions and exist as hydrate complex ions [*e.g.*,  $\text{Al}^{3+}(\text{H}_2\text{O})_3 \cdot x\text{H}_2\text{O}$ ], during electroplating under their high concentration or large current density, they existed as oxides in the resultant films instead of pure metals after their deposition from the solution. For instance, for  $\text{Al}^{3+}$  deposition, the electrochemical reaction was shown as follows:



(Note that the  $\text{Al}(\text{OH})_3$  gel was transformed into amorphous  $\text{AlO}_x$  after being dried).<sup>35</sup>

Due to the large different physical and chemical properties of  $\text{AlO}_x$  and  $\text{MnO}_y$  compared to FeCoNi, their presence during

**Table 1** Magnetic properties of FeNiCo films from types of additives

Additive	$H_{c\text{-easy}}/\text{Oe}$	$H_{c\text{-hard}}/\text{Oe}$	$B_s/\text{T}$	$H_k/\text{Oe}$	$\mu'_{\text{max}}$	$\mu''_{\text{max}}$	$f_r/\text{GHz}$	$\rho/\times 10^{-5}, \Omega \text{ cm}$
NA	$\geq 45$	$\geq 45$	$< 1.2$	150	393	184	3.8	1.8
SDS	45	36	1.85	80	143	98	3.6	6.0
SDS and B-reducer	8.0	7.1	2.43	55	1115	831	1.7	8.6
SDS, B-reducer and $\text{Al}^{3+}$	8.0	10.1	2.28	51	426	261	1.4	16.8
SDS, B-reducer and $\text{Mn}^{2+}$	17.5	14.1	2.30	50	511	645	0.6	11.1

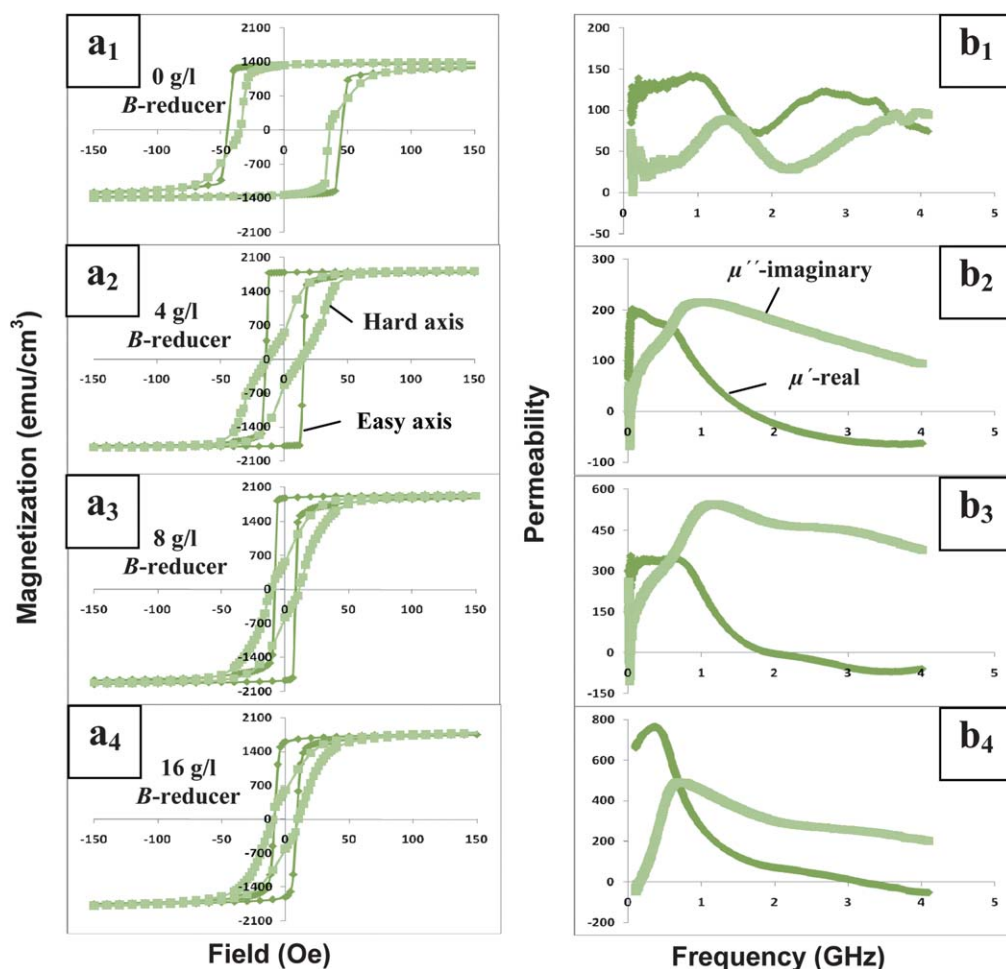


**Fig. 1** (a) *M*–*H* loops and (b) microwave permeability of the FeCoNi films electrodeposited on  $\text{SiO}_2$  from the solution containing  $1.1 \text{ g l}^{-1}$  of SDS and (1) 0, (2) 4, (3) 8, and (4)  $16 \text{ g l}^{-1}$  of *B*-reducer, respectively, at a current density of  $12 \text{ mA cm}^{-2}$ .

electrodeposition or minor doping resulted in the formation of numerous crystal defects in the FeCoNi alloy,<sup>19</sup> thus enhancing the FeCoNi growth in both in-plane and out-of-plane directions. As a result, the uniform nano-columnar granular FeCoNi films (shown in the following images) were formed. The films might contain low ratios of Al, Mn, and O atoms (depending on the additive concentration and plating current density). Accordingly, upon the subsequent addition of a small quantity of Al<sup>3+</sup> or Mn<sup>2+</sup> in the solution, Table 1 describes that the resistivity of the granular FeCoNi film was significantly increased to a value in the order of 10<sup>-4</sup> Ω cm. This is much higher than those of FeCoNi films reported from other solutions<sup>18</sup> and the resistivity could also be further increased to 10<sup>-3</sup> Ω cm by functionally doping more oxides. The resistivity is similar to that of semiconductor materials.<sup>2</sup> It is known that a higher resistivity of the magnetic films can reduce the effects of eddy-current by suppressing the eddy current and also increasing the skin depth during high frequency applications (*e.g.*, microwave absorption).<sup>1,2</sup>

### 3.2 Comparisons of the additive effects

Despite the atomic ratio in the FeCoNi film being largely decided by the plating current density and each salt concentration,<sup>16,22,23</sup> (instead of additives, as shown above), the organic and inorganic additives possessed different functions and effects in influencing the different properties of the deposited films. For detailed comparisons, Fig. 3a and b show the VSM and magnetic permeability results of the deposited films, respectively. The films were deposited from the plating solutions with different additives using the optimized concentrations and current densities. Under the optimized conditions, the largest permeability could be achieved

by using the same formula plating solution. Without using any additives, Fig. 3a<sub>1</sub> and b<sub>1</sub> show the prepared film having a large  $H_C$  of 51 Oe and a poor  $\mu$ - $f_r$  curve, respectively. After the addition of SDS,  $H_C$  of the film decreased to <50 Oe (shown in Fig. 1a<sub>1</sub>), while the film permeability remained low ( $\mu < 150$ ) (depicted in Fig. 1b<sub>1</sub> and Table 1). The shape of the poor permeability curve in Fig. 1b<sub>1</sub> is similar to that in Fig. 3b<sub>1</sub>, in which the real part of the permeability is much larger than the imaginary part when the resonance frequency  $f_r$  is less than 4.0 GHz, while they almost overlap when the  $f_r$  is more than 4.0 GHz. These curves suggest a poor film property for microwave absorption both before and after the addition of SDS. Upon subsequent addition of the  $B$ -reducer and electrodepositing at the optimized  $B$ -reducer concentration ( $\sim 9$  g l<sup>-1</sup>) and a current density of  $\sim 18$  mA cm<sup>-2</sup>, the  $H_C$  of the film decreased to 8 Oe (depicted in Fig. 3a<sub>2</sub>) and  $B_s$  increased to  $\sim 2.43$  T (shown in Table 1). In addition, the soft film (verified to be Fe<sub>48</sub>C<sub>50</sub>Ni<sub>2</sub> by EDX) displayed a large anisotropic field ( $H_k$ ) of  $\sim 52$  Oe. As compared to Fig. 1b, 2b, and 3b<sub>1</sub>, Fig. 3b<sub>2</sub> illustrates an increase in film permeability to the maximum values of 1115 and 831 for the real ( $\mu'$ ) and imaginary ( $\mu''$ ) part curves, respectively. This permeability value is much larger than those of reported monolayer films by means of sputtering, electrodeposition, or other methods.<sup>14,28,36,37</sup> Above the  $f_r$  ( $\sim 1.7$  GHz), the imaginary curve becomes much higher than the real curve up till the measurement limitation of the apparatus. These curves indicate that the film is potentially capable of absorbing microwaves effectively in a wide range of high frequencies. In particular, with the addition of SDS and  $B$ -reducer in the plating solution, the data in Table 1 show that the resistivity  $\rho$  of the prepared film was also increased, which was different from the scenario in which only the  $B$ -reducer was added.<sup>35</sup> The increased  $\rho$  is attributed to the effects

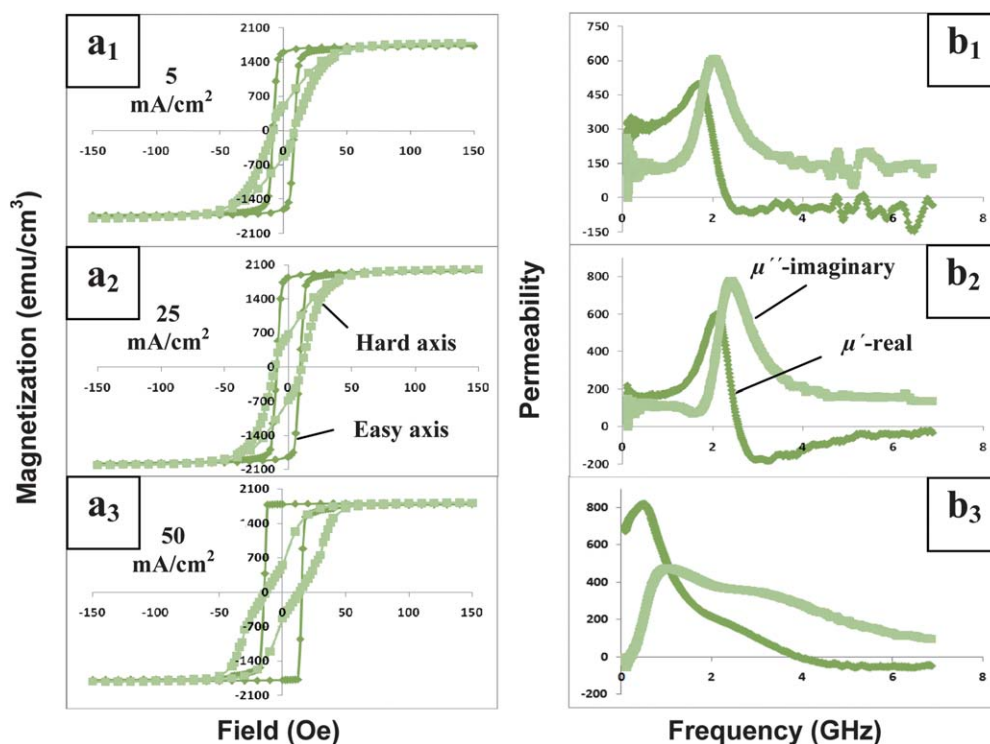


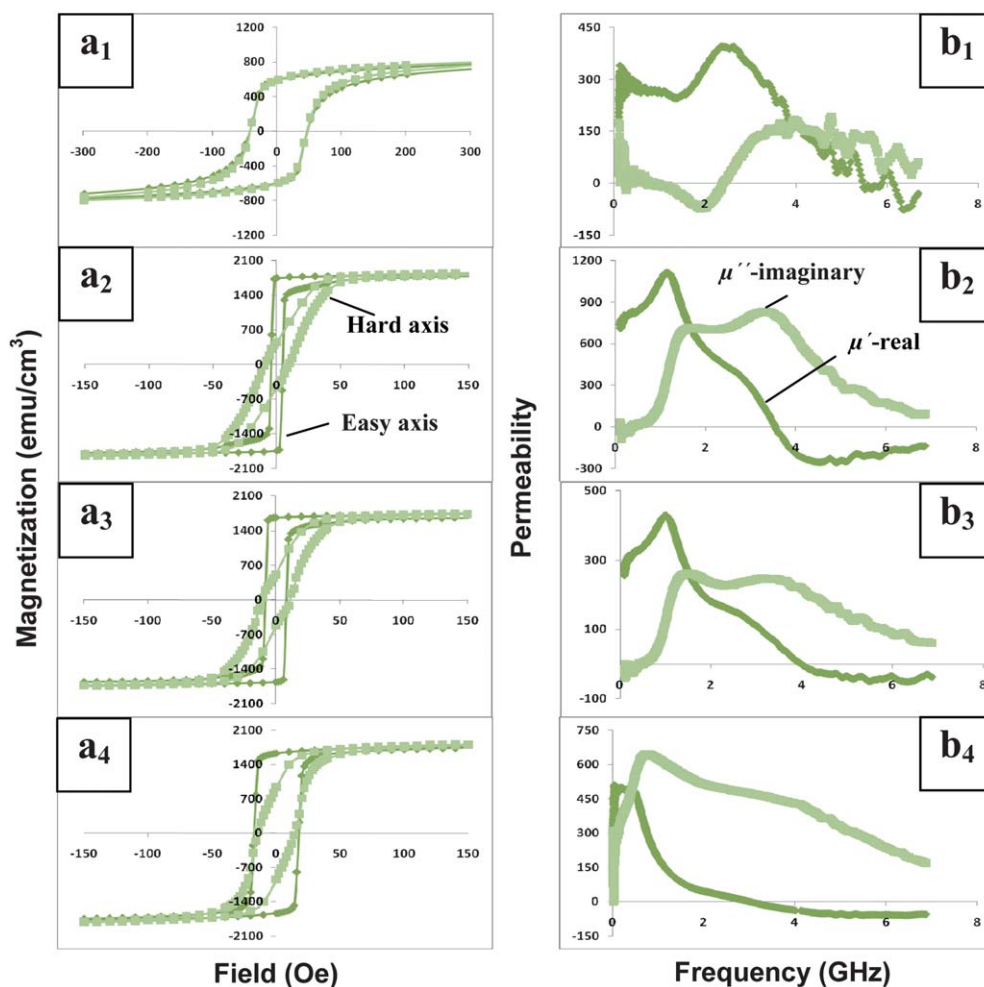
**Fig. 2** (a)  $M$ - $H$  loops and (b) microwave permeability of the FeCoNi films electrodeposited on glass from the solution which contains  $B$ -reducer of 8 g l<sup>-1</sup> at current densities of (1) 5, (2) 25, and (3) 50 mA cm<sup>-2</sup>, respectively.

of both the SDS and *B*-reducer additives, which changed the morphology of the prepared films (to be discussed in the following paragraph). Although the addition of a small quantity of  $\text{Al}^{3+}$  or  $\text{Mn}^{2+}$  into the plating solution led to a slight increase in  $H_c$ , and a slight decrease in  $B_s$  (Fig. 3a<sub>3</sub> and a<sub>4</sub>) and  $\mu$  (Fig. 3b<sub>3</sub> and b<sub>4</sub>), it significantly increased the  $\rho$  of the films (shown in Table 1). Moreover, the films were verified to have a very small magnetostriction of  $<10^{-5}$ . All these properties indicate that these films are very promising for the applications in a wide range of high frequency devices.

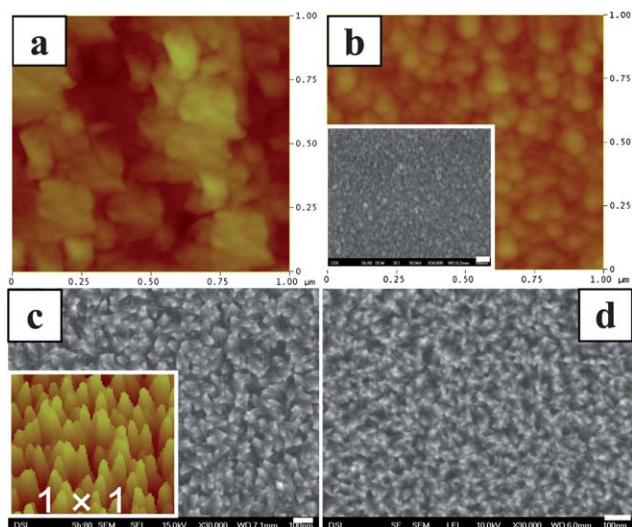
### 3.3 Morphology and texture structure of FeCoNi films

Fig. 4 shows the morphologies of the electrodeposited granular films with different additives. The film deposited from a solution without any additives obviously exhibited a non-uniform granular morphology (Fig. 4a). When viewed in a larger area of  $5 \times 5 \mu\text{m}^2$ , the surface of the film was micro-cracked. The morphology was the result of randomly mechanical-cracking due to the large build-up of internal stress within the film. After the addition of the SDS and *B*-reducer, the size of the granular particles in the  $\text{Fe}_{48}\text{Co}_{50}\text{Ni}_2$  film was reduced significantly and

became relatively uniform under the effects of the additives (mentioned above), as depicted in Fig. 4b. Thus, the exchange-coupling effects amongst the magnetic particles increased largely, which led to the decrease in  $H_c$  as well as the increase in  $B_s$ . This is similar to the situation when only the *B*-reducer was used as the additive.<sup>35</sup> Fig. 4c and d illustrate that with the further addition of  $\text{Al}^{3+}$  or  $\text{Mn}^{2+}$ , the columnar particles in the prepared films became more uniform despite a slight increase in the particle size. Because of a low quantity of  $\text{Al}^{3+}$  or  $\text{Mn}^{2+}$  addition and a moderate current density used in the plating, the prepared columnar films did not contain Al and Mn (from EDX results). Instead, the films were found to be doped with some oxygen, and the compositions were  $\text{Fe}_{46}\text{Co}_{49}\text{Ni}_1\text{O}_4$  and  $\text{Fe}_{46}\text{Co}_{50}\text{Ni}_1\text{O}_3$ , respectively. The uniform columnar particles and doped oxides led to the significant increase in the granular film resistivity. The reason is that the non-conductive metal oxides were formed and much more air (with a very high resistivity of  $3 \times 10^{15} \Omega \text{cm}$ ) was filled in the grain boundaries. As the formed oxides usually terminated the growth of FeCoNi crystals, when one FeCoNi column particle in the film was analyzed with EDX under a high FESEM magnification, the oxides were found to be mainly distributed at the particle boundary positions (shown in the



**Fig. 3** (a) *M*–*H* loops and (b) microwave permeability of the FeCoNi films electrodeposited on glass from the solutions (1) without additive, (2) with the additives of  $1.1 \text{ g l}^{-1}$  SDS and  $9 \text{ g l}^{-1}$  *B*-reducer, and further addition of (3)  $1.0 \text{ g l}^{-1}$   $\text{AlK}(\text{SO}_4)_2$  or (4)  $2.2 \text{ g l}^{-1}$   $\text{MnCl}_2$  at the respective optimal current densities of 15, 18, 14, and 16  $\text{mA cm}^{-2}$ .



**Fig. 4** AFM (a, b, and the inset of c) and FESEM (c, d and the inset of b) images of the FeCoNi films electrodeposited from the solutions: (a) without additive, (b) with the additives of  $1.1 \text{ g l}^{-1}$  SDS and  $9 \text{ g l}^{-1}$  B-reducer, (c) further addition of  $1.0 \text{ g l}^{-1}$   $\text{AlK}(\text{SO}_4)_2$ , or (d)  $2.2 \text{ g l}^{-1}$   $\text{MnCl}_2$  at current densities of 15, 18, 14, and  $16 \text{ mA cm}^{-2}$ , respectively. The inset of (c) is a 3 dimensional image of the film in (c). The scale bars of FESEM images are 100 nm.

Appendix). The non-conductive oxides at the grain boundaries could well form a resistive layer, which contributed to the increased film resistivity.

The XRD result in Fig. 5a shows the (110) texture structure of the columnar film, prepared from the plating solution containing SDS, B-reducer, and  $\text{Mn}^{2+}$  additives. Further investigation indicated that the similar texture structures [FeCoNi(110)] were displayed by all other thin FeCoNi nano-/micro-films, which were deposited from the plating solutions in the absence or presence of a small quantity of additives. These results revealed that the metal-crystal structure of the thin films depended largely on the structure of the seed layer [CoFe(110)]. However, the addition of too large a quantity of the additives [such as  $\text{AlK}(\text{SO}_4)_2 > 3 \text{ g l}^{-1}$  and  $\text{MnCl}_2 > 6 \text{ g l}^{-1}$ ] or applying a too high plating current density ( $> 50 \text{ mA cm}^{-2}$ ) could lead to amorphous particle films (shown in Fig. 5b). Furthermore, the resultant films were also doped with a high ratio of  $\text{AlO}_x$  or  $\text{MnO}_y$ , which led to the obvious decreases in microwave permeability and saturation

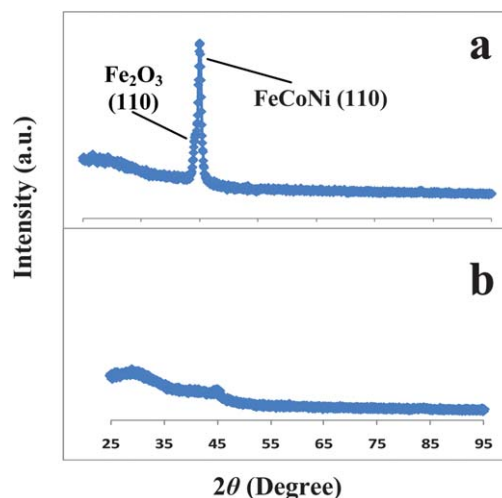


**Fig. 5**  $2\theta$  XRD results of  $0.6 \mu\text{m}$  (a)  $\text{Fe}_{46}\text{Co}_{50}\text{Ni}_1\text{O}_3$  and (b)  $\text{Fe}_{30}\text{Co}_{52}\text{Ni}_3\text{Mn}_1\text{O}_{14}$  films on 30 nm CoFe(110)/10 nm Ta/glass substrates. The films were deposited at current densities of 16 and  $70 \text{ mA cm}^{-2}$ , respectively, in the presence of SDS/B-reducer/ $\text{Mn}^{2+}$  additives.

flux density, despite a high resistivity (of the order of  $\sim 10^{-2} \Omega \text{ cm}$ ) being obtained.

#### 4. Conclusions

Soft magnetic FeCoNi based granular films were electrodeposited from cheap salt solutions. With the appropriate choices of organic and inorganic additives as well as plating parameters, the FeCoNi films, with a uniform nano-granular particulate morphology, were achieved with large magnetic microwave permeability, high resonance gigahertz frequency, as well as relatively high resistivity. These properties indicate that the fabricated films can be potentially used in the high-frequency applications of microwave absorption, magnetic data storage, portable wireless and biotechnology devices, *etc.*<sup>38</sup>

#### Appendix

Comparison of FeCoNi compositions at different film positions.

Note: the FeCoNi film was prepared from the solution containing  $1.1 \text{ g l}^{-1}$  SDS,  $9 \text{ g l}^{-1}$  B-reducer, and  $2.2 \text{ g l}^{-1}$   $\text{MnCl}_2$  at a current density of  $20 \text{ mA cm}^{-2}$ .

Position of analysis	Ratio of atom (%)			
	Fe	Co	Ni	O
Middle of one particle	45.4	48.2	1.3	5.1
Boundary of the particle	51.9	41.4	0.0	6.7
$10 \times 10 \mu\text{m}^2$ granular film	46.0	47.2	1.5	5.3

## Acknowledgements

The authors thank Mr S. H. Soh for the manpower support in this project.

## Notes and references

- 1 R. C. O'Handley, *Modern Magnetic Materials, Principles and Applications*, Wiley, New York, 2000.
- 2 Y. Liu, D. J. Sellmyer and D. Shindo, *Handbook of Advanced Magnetic Materials*, Spin 11097730, Tsinghua University Press, Springer, springeronline.com, 2006.
- 3 S. Azeemuddin, R. Divan, A. Hoffman and P. S. Wang, *Eur. J. Sci. Res.*, 2009, **32**, 141.
- 4 Y. Hsu, R. Fontana, M. Williams, P. Kasiraj, E. Lee and J. McCord, *J. Appl. Phys.*, 2001, **89**, 6808.
- 5 G. Zhang and L. R. Carley, *ISCAS (International Symposium on Circuits and Systems)*, 2004, **2004**, 469.
- 6 J. F. Wang, S. B. Qu, Z. T. Fu, H. Ma, Y. M. Yang, X. Wu, Z. Wu and M. J. Hao, *Prog. Electromagn. Res. Lett.*, 2009, **7**, 15.
- 7 M. Gillick, I. D. Robertson and J. S. Joshi, *IEEE Trans. Microwave Theory Tech.*, 1993, **41**, 1606.
- 8 M. Vroubel, Y. Zhuang, B. Rejaei, J. N. Burghartz, A. M. Crawford and S. X. Wang, *IEEE Trans. Magn.*, 2004, **40**, 2835.
- 9 L. H. Chen, T. J. Klemmer, K. A. Ellis, R. B. van Dover and S. Jin, *J. Appl. Phys.*, 2000, **87**, 5858.
- 10 Y. Zhuang, B. Rejaei, E. Boellaard, M. Vroubel and J. N. Burghartz, *IEEE Electron Device Lett.*, 2003, **24**, 224.
- 11 J. X. Qiu, H. G. Shen and M. Y. Gu, *Powder Technol.*, 2005, **154**, 116.
- 12 S. X. Wang, N. X. Sun, M. Yamaguchi and S. Yabukami, *Nature*, 2000, **407**, 150.
- 13 J. H. Oh, K. S. Oh, C. G. Kim and C. S. Hong, *Composites, Part B*, 2004, **35**, 49.
- 14 W. C. Hsu, S. C. Chen and P. C. Kuo, *Mater. Sci. Eng., B*, 2004, **111**, 142.
- 15 G. R. Amiri, M. H. Yousefi, M. R. Abolhassani, S. Manouchehri, M. H. Keshavarz and S. Fatahian, *J. Magn. Magn. Mater.*, 2011, **323**, 730.
- 16 B. Y. Zong, G. C. Han, Y. K. Zheng, Z. B. Guo, K. B. Li, L. Wang, J. J. Qiu, Z. Y. Liu, L. H. An, P. Luo, H. L. Li and B. Liu, *IEEE Trans. Magn.*, 2006, **42**, 2775.
- 17 Y. H. Wu, B. J. Yang, B. Y. Zong, H. Sun, Z. X. Shen and Y. P. Feng, *J. Mater. Chem.*, 2004, **14**, 469.
- 18 E. I. Cooper, C. Bonhôte, J. Heidmann, Y. Hsu, P. Kern, J. W. Lam, M. Ramasubramanian, N. Robertson, L. T. Romankiw and H. Xu, *IBM J. Res. Dev.*, 2005, **49**, 103.
- 19 S. Sahoo, B. C. Ray and A. Mallik, *Sono-Electrodeposition of Thin Films*, LAP Lambert Academic Publishing, AG & Co KG, ISBN: 9783843362658, 2010.
- 20 F. M. F. Rhen and S. Roy, *IEEE Trans. Magn.*, 2008, **44**, 3917.
- 21 S. Mizutani, T. Yokoshima, H. S. Nam, T. Nakanishi, T. Osaka and Y. Yamazaki, *IEEE Trans. Magn.*, 2000, **36**, 2539.
- 22 T. Osaka, M. Takai, K. Hayashi, K. Ohashi, M. Saito and K. Yamada, *Nature*, 1998, **392**, 796.
- 23 S. H. Liao, *IEEE Trans. Magn.*, 1987, **23**, 2981.
- 24 S. R. Brankovic, X. Yang, T. J. Klemmer and M. Seigler, *IEEE Trans. Magn.*, 2006, **42**, 132.
- 25 T. Osaka, T. Yokoshima, D. Shiga, K. Imai and K. Takashima, *Electrochem. Solid-State Lett.*, 2003, **6**, C53.
- 26 X. M. Liu, J. O. Rantschler, C. Alexander and G. Zangari, *IEEE Trans. Magn.*, 2003, **39**, 2362.
- 27 S. S. Kim, S. T. Kim, J. M. Ahn and K. H. Kim, *J. Magn. Magn. Mater.*, 2004, **271**, 39.
- 28 B. Gao, L. Qiao, J. B. Wang, Q. F. Liu, F. S. Li, J. Feng and D. S. Xue, *J. Phys. D: Appl. Phys.*, 2008, **41**, 1.
- 29 W. B. Chen, M. G. Han and L. J. Deng, *PIERS Online*, 2010, **6**, 1.
- 30 Y. P. Wu, G. C. Han and L. B. Kong, *J. Magn. Magn. Mater.*, 2010, **322**, 3223.
- 31 S. Masakatsu and I. Osamu, *IEEE Trans. Magn.*, 1994, **30**, 155.
- 32 H. Greve, C. Pochstein, H. Takeleh and V. Zaporojtchenko, *Appl. Phys. Lett.*, 2006, **89**, 242501.
- 33 B. Y. Zong, G. C. Han, J. J. Qiu, Z. B. Zai, L. Wang, W. K. Yeo and B. Liu, *Res. Lett. Phys. Chem.*, 2008, **2008**, 1, DOI: 10.1155/2008/342976.
- 34 T. Homma, H. Nakai, M. Onishi and T. Osaka, *J. Phys. Chem. B*, 1999, **103**, 1774.
- 35 F. Endres, D. MacFarlane and A. Abbott, *Electrodeposition From Ionic Liquids*, Wiley-VCH, 2008, www.books.google.com.
- 36 H. P. Lu, J. Yang and L. J. Deng, *PIERS Online*, 2010, **6**, 105.
- 37 L. W. Deng, B. Y. Huang, W. S. Liu, K. S. Zhou and B. C. Yang, *Trans. Nonferrous Met. Soc. China*, 2009, **19**, s734.
- 38 R. C. Che, L. M. Peng, X. F. Duan, Q. Chen and X. L. Liang, *Adv. Mater.*, 2004, **16**, 401.